Quasiparticle Interference of C_2-Symmetric Surface States in a LaOFeAs Parent Compound

Xiaodong Zhou,[1] Cun Ye,[1] Peng Cai,[1] Xiangfeng Wang,[2] Xianhui Chen,[2] and Yayu Wang[1,*]

[1]*Laboratory of Low Dimensional Quantum Physics, Department of Physics, Tsinghua University, Haidian, Beijing 100084, People's Republic of China*

[2]*Hefei National Laboratory for Physical Science at Microscale and Department of Physics, University of Science and Technology of China, Hefei, Anhui 230026, People's Republic of China*

(Received 1 September 2010; published 22 February 2011)

We present scanning tunneling microscopy studies of the LaOFeAs parent compound of iron pnictide superconductors. High resolution spectroscopic imaging reveals strong standing wave patterns induced by quasiparticle interference of two-dimensional surface states. Fourier analysis shows that the distribution of scattering wave vectors exhibits pronounced twofold (C_2) symmetry, strongly reminiscent of the nematic electronic state found in $CaFe_{1.94}Co_{0.06}As_2$. The implications of these results to the electronic structure of the pnictide parent states will be discussed.

DOI: 10.1103/PhysRevLett.106.087001 PACS numbers: 74.70.Xa, 73.20.At, 74.55.+v

The recently discovered iron-based (pnictide) superconductors [1] with T_c up to 55 K bring new hope for unveiling the mystery of high T_c superconductivity, which has puzzled the physics community for more than two decades since the discovery of copper oxide (cuprate) superconductors. The pnictides share many similarities with the cuprates, such as the quasi-two-dimensional layered structures and electron conduction via $3d$ electronic states. More interestingly, the parent compounds of the pnictides are also antiferromagnetically (AF) ordered [2], just like that of the cuprates. Superconductivity emerges when doped charge carriers destroy the long-range AF ordering. The apparently close ties between the AF and superconducting phases have prompted the proposals of magnetically mediated pairing as a promising mechanism of high T_c superconductivity in the pnictides [3–5]. To test the validity of various theories, it is imperative to elucidate the electronic structure of the parent compound. A remarkable recent discovery along this direction is the quasi-one-dimensional (1D) liquid-crystal–like electronic nanostructures found in $CaFe_{1.94}Co_{0.06}As_2$ parent state by scanning tunneling microscopy (STM) [6]. This "nematic" electronic structure has also been shown to be a key phenomenon in the cuprates, and has been suspected to be essential to the origin of high T_c superconductivity [7,8].

Whether the electronic nematicity is a universal feature of the pnictides and what is the physical mechanism behind it are still under heated debate [9–12]. Much theoretical attention has been paid to the 1111 family ReOFeAs (Re = rare earth elements) [3,4,9,13], which have the highest T_c among all pnictides. However, the nanoscale electronic structure of 1111 parent compounds is still unknown, despite numerous STM studies on the pnictides [14–21]. In this Letter we present the first atomic scale STM studies of LaOFeAs parent compound. High resolution spectroscopic imaging reveals strong quasiparticle interference (QPI) patterns induced by surface electronic states. The C_2 symmetry of the $\mathbf{q}$-space structure is closely analogous to that found in the 122 compound [6], suggesting that it is a universal feature of the pnictide parent states. However, the C_2-symmetric QPI pattern is observed only on the LaO layer, but not the FeAs layer as seen in the 122 compound [6]. The QP dispersions in the two systems are also drastically different. These discrepancies suggest that the mechanism of the C_2-symmetric electronic structure needs to be further investigated.

High quality LaOFeAs single crystals are grown with NaAs flux method as described elsewhere [22]. Resistivity measurement shows a transition into the AF state at $T_N \sim 140$ K. For STM experiments, LaOFeAs single crystals are cleaved at 77 K in ultrahigh vacuum (UHV) and then immediately transferred into the STM stage, which stays at 5 K in UHV. All data reported here are obtained at 5.0 K. The dI/dV spectra are acquired by a standard lock-in technique with modulation frequency $f = 223$ Hz.

Figure 1(a) shows a 400 Å × 400 Å topographic image of cleaved LaOFeAs, which reveals two types of clean and

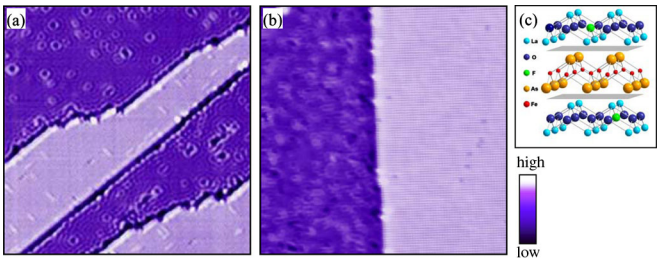

FIG. 1 (color online). (a) 400 Å × 400 Å constant current image of the cleaved surface of parent LaOFeAs taken with sample bias $V = -100$ mV and tunneling current $I = 20$ pA. Two different types of surfaces are revealed. (b) 400 Å × 400 Å constant current image of F-doped $LaO_{0.9}F_{0.1}FeAs$ taken with $V = -100$ mV and $I = 100$ pA. (c) Schematic crystal structure of LaOFeAs with O partially substituted by F.

flat surfaces. The higher terrace here has a well-resolved lattice structure, while the lower terrace shows strong standing waves around impurities and along step edges. The two unequivalent surfaces are expected from the LaOFeAs crystal structure, as illustrated in Fig. 1(c). LaOFeAs consists of alternatively stacked LaO and FeAs layers. The crystal cleaves easily between the layers [gray planes in Fig. 1(c)], leading to the exposure of As-terminated FeAs layer and La-terminated LaO layer with equal possibilities. To distinguish the two surfaces experimentally, we compare the STM topography of the parent LaOFeAs [Fig. 1(a)] with that of F-doped $LaO_{0.9}F_{0.1}FeAs$ [Fig. 1(b)]. F dopants are expected to create disorders in the LaO layer but leave the FeAs layer intact. Indeed, the surface with standing waves in Fig. 1(b) is much more disordered than that in Fig. 1(a), and thus can be identified as the LaO layer. The atomically sharp surface in Fig. 1(b) is unaffected by F doping, thus can be identified as the FeAs layer. More STM images supporting this layer identification are shown in the supplemental materials [23].

Figure 2(a) is a 200 Å × 200 Å topographic image of the FeAs surface, which has a clear atomic lattice decorated with cigar-shaped defects of unknown origin. The high-resolution image of a defect free area [Fig. 2(a), inset] shows that the lattice has a nearly square symmetry with lattice constant around 4.0 Å, in good agreement with the distance between neighboring As atoms [2]. We note that

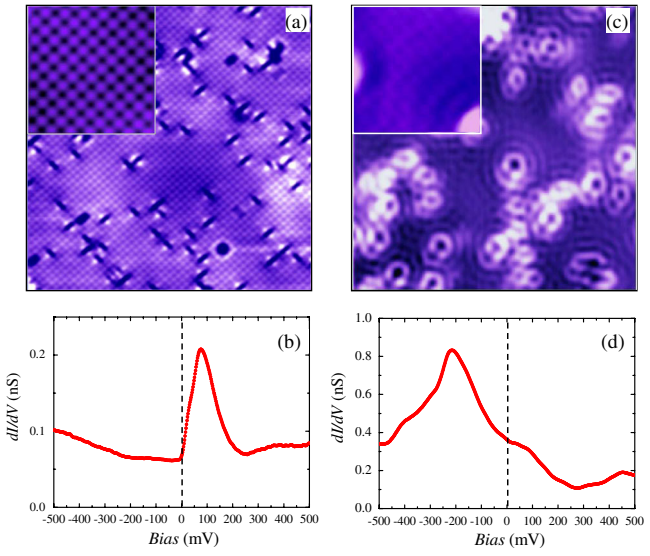

FIG. 2 (color online). (a) 200 Å × 200 Å topography of the FeAs surface taken with $V = 100$ mV and $I = 50$ pA. (Inset) 40 Å × 40 Å close-up image shows clear atomic lattice with 4 Å lattice constant. (b) dI/dV of the FeAs surface has a peak at positive sample bias around +100 mV. (c) 200 Å × 200 Å topography of the LaO surface taken with $V = -100$ mV and $I = 40$ pA displays strong standing waves around scattering centers. (Inset) 40 Å × 40 Å image shows the atomic lattice. (d) dI/dV of the LaO surface has a peak at negative sample bias around −200 mV.

currently our STM cannot resolve the ~1% lattice distortion because it is beyond the accuracy of the piezoelement calibration. Figure 2(b) shows the dI/dV spectrum of the FeAs surface taken on a defect free region. The curve peaks sharply at positive bias $V = +100$ mV, indicating a large density of state (DOS) in the unoccupied state. The distinct peak is a highly reproducible and uniform feature of the FeAs surface. It may reflect the hole excess (electron deficiency) of the exposed FeAs layer due to the polar surface character of cleaved LaOFeAs [24], but its exact origin is still unknown.

Figure 2(c) is a 200 Å × 200 Å topographic image of the LaO surface. The most striking feature here is the existence of strong standing waves around impurity centers. The amplitude of the standing waves decays rapidly from the impurities. At relatively clean areas between impurities, the atomic lattice can still be resolved, as shown in Fig. 2(c), inset. The lattice also has a nearly square symmetry with lattice constant ~4.0 Å. Figure 2(d) shows the dI/dV spectrum taken at locations away from impurities. In contrast to that of the FeAs surface, the spectrum here has a peak at negative bias $V = -200$ mV, implying a large DOS in the occupied state most likely due to the electron excess of the exposed LaO layer as a result of polar surface. The peak feature is also highly reproducible and uniform in space, but it is unclear if it is closely related to the standing wave patterns.

The standing waves in the LaO surface are induced by the scattering interference of QPs, as has been observed in various metal [25], semiconductor [26], and superconductor surfaces [27]. The interference between incident electron wave with wave vector $\mathbf{k}_i$ and elastically scattered electron wave $\mathbf{k}_f$ induces a spatial DOS oscillation with wave vector $\mathbf{q} = \mathbf{k}_f - \mathbf{k}_i$ and wavelength $\lambda = 2\pi/q$. Since the wave vector $\mathbf{q}$ contains important $\mathbf{k}$-space information, the QPI imaging technique has become a powerful tool for studying the Fermi surface geometry and dispersion relation of novel materials [28,29].

To extract the $\mathbf{k}$-space information from QPI, we take a series of differential conductance maps $dI/dV(\mathbf{r}, V)$ at different bias voltages V, as shown in the upper panels of Fig. 3. The standing waves in each map correspond to the QPI of electrons with selected energy $\varepsilon = eV$. Both the wavelength and spatial pattern of QPI evolve with ε, manifesting the dispersion of QPs. The lower panels of Fig. 3 show the Fourier transformed (FT) conductance maps $dI/dV(\mathbf{q}, V)$, which illustrate the $\mathbf{q}$-space structure of QPI. The nearly square atomic lattice renders four sharp Bragg peaks (surrounded by gray circles) with fixed wave vector $q_0 = 2\pi/4$ Å. The $\mathbf{q}$ wave vectors responsible for the QPI, on the other hand, are the broad features that disperse with energy.

The most striking feature revealed by the FT maps is the pronounced C_2 symmetry exhibited by the distribution of scattering wave vectors. The dominant $\mathbf{q}$ points are

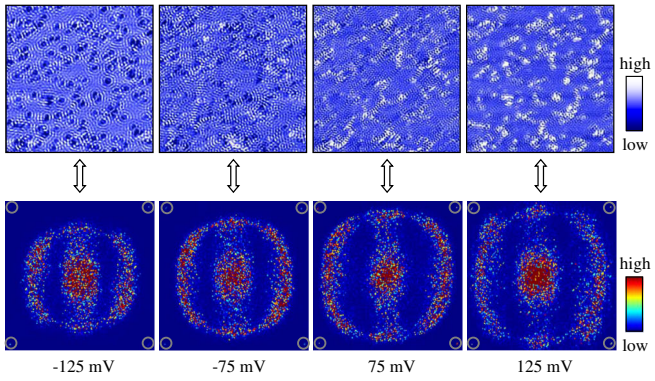

FIG. 3 (color online). (upper panel) Differential conductance maps $dI/dV(\mathbf{r}, V)$ over a 400 Å × 400 Å area on the LaO surface taken with sample bias −125 mV, −75 mV, 75 mV, and 125 mV. (lower panel) Fourier transformed conductance maps $dI/dV(\mathbf{q}, V)$ reveal that the $\mathbf{q}$-space structure of QPI exhibits pronounced C_2 symmetry.

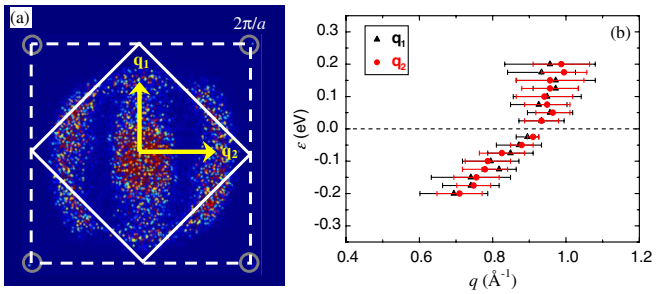

FIG. 4 (color online). (a) The $\mathbf{q}$ map taken at −125 mV with respect to the Brillouin zone of LaOFeAs. The broken (solid) square indicates the unreconstructed (reconstructed) BZ. The dominant $\mathbf{q}$ wave vectors are distributed along the Fe-Fe bond direction. The Bragg peaks with $q_0 = 2\pi/a = 2\pi/4$ Å are circled in gray. (b) The ε vs q dispersions for the two $\mathbf{q}$ wave vectors along the Fe-Fe bond directions as indicated by arrows in (a).

distributed along two vertical arcs in the present orientation, apparently breaking the C_4 symmetry. Similarly, there are slightly weaker $\mathbf{q}$ points in the central strip along the vertical direction, but not along the horizontal direction. To identify the orientation of the $\mathbf{q}$ vectors, the $\mathbf{q}$ map taken at $\varepsilon = -125$ meV is plotted in Fig. 4(a) with respect to the Brillouin zone (BZ). The broken square indicates the unreconstructed BZ and the solid square indicates the reconstructed BZ of the parent state. By comparing with the Bragg peaks, we found that the arcs with dominant $\mathbf{q}$ points are aligned along the Fe-Fe bond direction, although we cannot distinguish the orthorhombic a and b axis. The overall feature bears a strong resemblance to the $\mathbf{q}$ maps of the nematic electronic state in the 122 parent $CaFe_{1.94}Co_{0.06}As_2$ [6].

The QPI shown above are induced by 2D surface states because the standing waves are so pronounced that the atomic lattices are almost concealed. Similar behavior has been found only in materials with well-defined 2D surface electronic structures [25,26]. The QPI of the bulk states usually shows much weaker features that can only be visualized when the lattice effect is removed [6]. Surface states on cleaved 1111 pnictides were first hinted by angle resolved photoemission spectroscopy (ARPES), which found extra large hole pocket around the Γ point incompatible with bulk band structure [30–32]. Density functional theory (DFT) calculations also suggest the formation of 2D surface states on the highly polar surfaces of cleaved LaOFeAs, with electronlike surface band on LaO and holelike surface band on FeAs [33]. Recent ARPES data provide direct evidence for the existence of surface states by showing the lack of k_z dispersion for certain bands on cleaved LaOFeAs [34,35].

The surface state QPI observed on the LaO surface can be directly compared with the local-density approximation (LDA) and ARPES results. Figure 4(b) displays the $\varepsilon - q$ dispersions extracted from the FT-QPI maps. The QPs exhibit electronlike dispersion along both Fe-Fe orthorhombic directions, consistent with the electronlike surface band on the LaO surface predicted by LDA. At the Fermi level ($\varepsilon = 0$), the QPI wave vector is estimated to be $q_F = 0.92$ Å^{-1}. Assuming intraband backscattering as the dominant scattering mechanism so that $q_F = 2k_F$, this renders a Fermi momentum $k_F = 0.46$ Å^{-1}, in quantitative agreement with the ARPES measured $k_F = 0.45$ Å^{-1} for the electronlike λ_{s2} band on LaO [35].

Although the symmetry of the electronic structure is the same for LaOFeAs and $CaFe_{1.94}Co_{0.06}As_2$, the dispersion relations are drastically different. In $CaFe_{1.94}Co_{0.06}As_2$ the electronic structure is static along the orthorhombic a axis and dispersive along the b axis [6]. In LaOFeAs the QPs are dispersive along both orthorhombic directions, as shown in Fig. 4(b). The dispersion behavior has important implications for the physical mechanism of the observed C_2 symmetry. The quasi-1D liquid-crystal–like nematic ordering found in $CaFe_{1.94}Co_{0.06}As_2$ is more consistent with the melted stripes picture [36]. The dispersive QPs observed here on LaOFeAs suggest that the Pomeranchuk instability picture of spontaneous distortion of Fermi surface may be more relevant [11]. Moreover, the C_2 symmetry of QPI may simply arise from C_2-symmetric band structure (due to the stripelike AF ordering) [37] or a scattering potential with C_2 symmetric structure factors [38]. In-depth theoretical analysis of the QPI spectrum based on realistic band structures for specific materials is imperative to distinguish the various mechanisms.

It is more surprising that the FeAs layer of LaOFeAs does not exhibit any characteristic electronic nanostructure despite intensive search [23]. First, the holelike surface state suggested by LDA and ARPES is not observed by STM. One possible explanation is that the wave function of the excess hole on FeAs may hybridize strongly with that of the bulk states penetrating the FeAs layer.

This hybridization leads to a holelike band structure much less 2D than a surface state band. The k_z dispersion may still be weak, but the surface state QPI pattern completely vanishes. Second, the liquid-crystal–like nematic ordering found in $CaFe_{1.94}Co_{0.06}As_2$ is not seen on the FeAs surface of LaOFeAs either. However, we cannot exclude its existence at this stage because the quality of our current sample may not be good enough to allow us to reveal such weak features on the FeAs surface. Therefore the results reported here are not straightforward to investigate the FeAs layer, although the LaO layer would reflect the bulk properties thus involving the effects of the FeAs layer.

In summary, STM studies on LaOFeAs parent compound reveal QPI patterns with the C_2 symmetry strikingly similar to that in $CaFe_{1.94}Co_{0.06}As_2$. The existence of C_2 symmetric electronic states in two different pnictide families strongly suggests that it is a universal feature of the pnictide parent state. However, apparent discrepancies do exist between the two compounds, especially the absence of C_2-symmetric electronic state on the FeAs layer of LaOFeAs. Since the FeAs layer is the common structure of many pnictides and is expected to be essential for the superconductivity, it is highly desired to elucidate its local electronic structure by future STM studies on much cleaner LaOFeAs crystals.

We thank D. L. Feng, J. P. Hu, D. H. Lu, Z. Y. Weng, C. K. Xu, H. Yao, H. Zhai, and X. J. Zhou for helpful discussions. This work is supported by the National Natural Science Foundation of China and by the Ministry of Science and Technology of China (Grants No. 2009CB929402, No. 2010CB923003, and No. 2011CBA00101).

*yayuwang@tsinghua.edu.cn

[1] K. Ishida, Y. Nakai, and H. Hosono, J. Phys. Soc. Jpn. **78**, 062001 (2009).
[2] C. de la Cruz *et al.*, Nature (London) **453**, 899 (2008).
[3] I. I. Mazin *et al.*, Phys. Rev. Lett. **101**, 057003 (2008).
[4] K. Kuroki *et al.*, Phys. Rev. Lett. **101**, 087004 (2008).
[5] F. Wang *et al.*, Phys. Rev. Lett. **102**, 047005 (2009).
[6] T. M. Chuang *et al.*, Science **327**, 181 (2010).
[7] S. A. Kivelson, E. Fradkin, and V. J. Emery, Nature (London) **393**, 550 (1998).
[8] V. J. Emery, S. A. Kivelson, and J. M. Tranquada, Proc. Natl. Acad. Sci. U.S.A. **96**, 8814 (1999).
[9] X. H. Chen *et al.*, Nature (London) **453**, 761 (2008).
[10] C. Xu, M. Müller, and S. Sachdev, Phys. Rev. B **78**, 020501(R) (2008).
[11] H. Zhai, F. Wang, and D. H. Lee, Phys. Rev. B **80**, 064517 (2009).
[12] W. C. Lee, and C. J. Wu, Phys. Rev. Lett. **103**, 176101 (2009).
[13] T. Yildirim, Phys. Rev. Lett. **101**, 057010 (2008).
[14] F. Massee *et al.*, Phys. Rev. B **79**, 220517 (2009).
[15] V. B. Nascimento *et al.*, Phys. Rev. Lett. **103**, 076104 (2009).
[16] Y. Yin *et al.*, Phys. Rev. Lett. **102**, 097002 (2009).
[17] F. C. Niestemski*et al.*, arXiv:0906.2761.
[18] T. Hanaguri *et al.*, Science **328**, 474 (2010).
[19] H. Zhang *et al.*, Phys. Rev. B **81**, 104520 (2010).
[20] L. Shan *et al.*, arXiv:1005.4038.
[21] G. R. Li *et al.*, arXiv:1006.5907.
[22] J. Q. Yan *et al.*, Appl. Phys. Lett. **95**, 222504 (2009).
[23] See supplemental material at http://link.aps.org/supplemental/10.1103/PhysRevLett.106.087001 for the layer identification method and topographic images on the FeAs layer taken at different biases.
[24] N. Nakagawa, H. Y. Hwang, and D. A. Muller, Nature Mater. **5**, 204 (2006).
[25] M. F. Crommie, C. P. Lutz, and D. M. Eigler, Nature (London) **363**, 524 (1993).
[26] K. Kanisawa *et al.*, Phys. Rev. Lett. **86**, 3384 (2001).
[27] J. E. Hoffman *et al.*, Science **297**, 1148 (2002).
[28] L. Petersen *et al.*, J. Electron Spectrosc. Relat. Phenom. **109**, 97 (2000).
[29] K. McElroy *et al.*, Nature (London) **422**, 592 (2003).
[30] D. H. Lu *et al.*, Physica (Amsterdam) **469C**, 452 (2009).
[31] C. Liu *et al.*, Physica (Amsterdam) **469C**, 491 (2009).
[32] H. Y. Liu *et al.*, Phys. Rev. Lett. **105**, 027001 (2010).
[33] H. Eschrig, A. Lankau, and K. Koepernik, Phys. Rev. B **81**, 155447 (2010).
[34] C. Liu *et al.*, Phys. Rev. B **82**, 075135 (2010).
[35] L. X. Yang *et al.*, Phys. Rev. B **82**, 104519 (2010).
[36] E. Fradkin and S. A. Kiverlson, Science **327**, 155 (2010).
[37] J. Knolle *et al.*, Phys. Rev. Lett. **104**, 257001 (2010).
[38] L. Capriotti, D. J. Scalapino, and R. D. Sedgewick, Phys. Rev. B **68**, 014508 (2003).